

## Supporting Information

Syntheses, structures and catalytic activity of tetranuclear Mg complexes in the  
ROP of cyclic esters under industrial relevant conditions

*Swarup Ghosh, Christoph Wölper, Alexander Tjaberings, André H. Gröschel, Stephan Schulz\**

## Content

### I. Characterization of 1-4

**Figures S1-S3.**  $^1\text{H}$ ,  $^{13}\text{C}$  NMR and IR spectra of **1**.

**Figures S4-S6.**  $^1\text{H}$ ,  $^{13}\text{C}$  NMR and IR spectra of **2**.

**Figures S7-S9.**  $^1\text{H}$ ,  $^{13}\text{C}$  NMR and IR spectra of **3**.

**Figures S10-S12.**  $^1\text{H}$ ,  $^{13}\text{C}$  NMR and IR spectra of **4**.

**Figure S9-S12.** IR spectra of **1-4**.

**Figures S13-S16.** DOSY NMR spectra of **1-4**.

### II. Crystallographic Details

**Table S1.** Crystal data for compound **1**, **2**[thf]<sub>2</sub>, **3**[thf]<sub>2</sub> and **4**[thf]<sub>2</sub>.

**Table S2.** Mg-O and Mg-N bond lengths as well as O-Mg-O and Mg-O-Mg bond angles of compound **1**, **2**[thf]<sub>2</sub>, **3**[thf]<sub>2</sub> and **4**[thf]<sub>2</sub>.

### III. Polymerization Studies

**Figure S17.** Homonuclear decoupled  $^1\text{H}$ -NMR spectrum of *rac*-PLA in  $\text{CDCl}_3$  (methine H-atom region) obtained by reaction of *rac*-LA and **1** in ratio 200:1 at 140 °C.

**Figure S18.** Homonuclear decoupled  $^1\text{H}$ -NMR spectrum of *rac*-PLA in  $\text{CDCl}_3$  (methine H-atom region) obtained by reaction of *rac*-LA and **2** in ratio 200:1 at 140 °C.

**Figure S19.** Homonuclear decoupled  $^1\text{H}$ -NMR spectrum of *L*-PLA in  $\text{CDCl}_3$  (methine H-atom region) obtained by reaction of *L*-LA and **1** in ratio 200:1 at 140 °C.

**Figure S20.**  $^1\text{H}$ -NMR spectrum of *rac*-PLA in  $\text{CDCl}_3$  obtained by reaction of *rac*-LA and **1** in ratio 50:1 at 140 °C.

**Figure S21.** MALDI-TOF spectrum of *rac*-PLA obtained by reaction of *rac*-LA and **1** (50:1) at 140 °C.

**Figure S22.**  $^1\text{H}$ -NMR spectrum of  $\epsilon$ -PCL in  $\text{CDCl}_3$  obtained by reaction of  $\epsilon$ -CL and **1** (50:1) at 80 °C.

**Figure S23.** MALDI-TOF spectrum of  $\epsilon$ -PCL in  $\text{CDCl}_3$  obtained by reaction of  $\epsilon$ -CL and **1** (50:1) at 80 °C

**Figure S24.**  $^1\text{H}$ -NMR spectrum of *rac*-PLA in  $\text{CDCl}_3$  obtained by reaction of *rac*-LA and **1** in the presence of benzyl alcohol as a co-initiator (50:1:2) at 140 °C.

**Figure S25.** MALDI-TOF spectrum of *rac*-PLA in  $\text{CDCl}_3$  obtained by reaction of *rac*-LA and **1** in the presence of benzyl alcohol as a co-initiator (50:1:2) at 140 °C.

**Figure S26.**  $^1\text{H}$ -NMR spectrum of  $\epsilon$ -PCL in  $\text{CDCl}_3$  obtained by reaction of  $\epsilon$ -CL and **1** in the presence of benzyl alcohol as a co-initiator (50:1:2) at 80 °C.

**Figure S27.** MALDI-TOF spectrum of  $\epsilon$ -PCL in  $\text{CDCl}_3$  obtained by reaction of  $\epsilon$ -CL and **1** in the presence of benzyl alcohol as a co-initiator (50:1:2) at 80 °C.

**Figure 28.** IR spectrum of *rac*-PLA obtained by reaction of *rac*-LA and **1** in 50:1 molar ratio at 140 °C.

**Figure 29.** IR spectrum of  $\epsilon$ -PCL obtained by reaction of  $\epsilon$ -CL and **1** in 50:1 molar ratio at 80 °C.

**Figure 30.** GPC diagram of *rac*-PLA obtained by reaction of *rac*-LA and **1** in 2000:1 molar ratio at 140 °C.

**Figure 31.** GPC diagram of *rac*-PLA obtained by reaction of *rac*-LA and **1** in 10000:1 molar ratio at 140 °C.

**Figure 32.** GPC diagram of  $\epsilon$ -PCL obtained by reaction of  $\epsilon$ -CL and **1** in 5000:1 molar ratio at 80 °C.

**Figure 33.** GPC diagram of  $\epsilon$ -PCL obtained by reaction of  $\epsilon$ -CL and **1** in 10000:1 molar ratio at 80 °C.

**Table S3.** Polymerization data for *rac*-LA and  $\epsilon$ -CL with **1-4** with BnOH as an initiator (200:1:4) under the solvent free condition.

**Table S4.** Polymerization data of *rac*-LA and  $\epsilon$ -CL using catalyst **1** with varying  $[M]_0/[C]_0$ .

**Figure S1.**  $^1\text{H}$  NMR (300 MHz,  $\text{CDCl}_3$ , 25  $^\circ\text{C}$ ) spectrum of **1**.

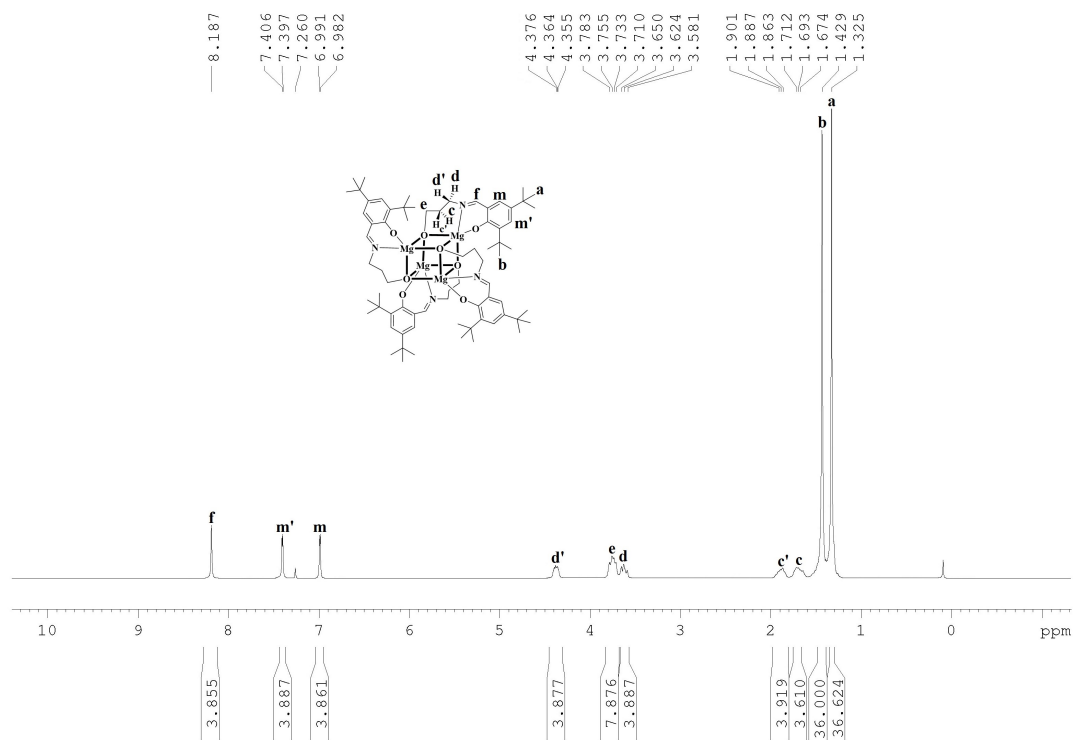


**Figure S2.**  $^{13}\text{C}$  NMR (75 MHz,  $\text{CDCl}_3$ , 25  $^\circ\text{C}$ ) spectrum of **1**.

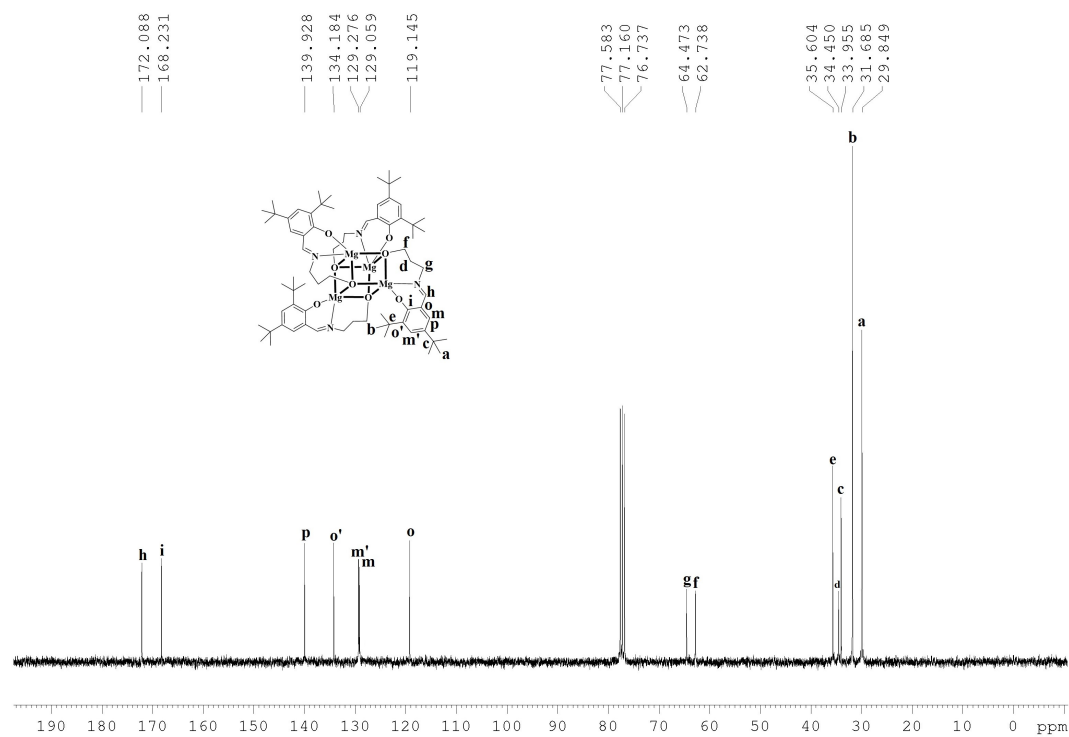


Figure S3. IR spectrum of 1.

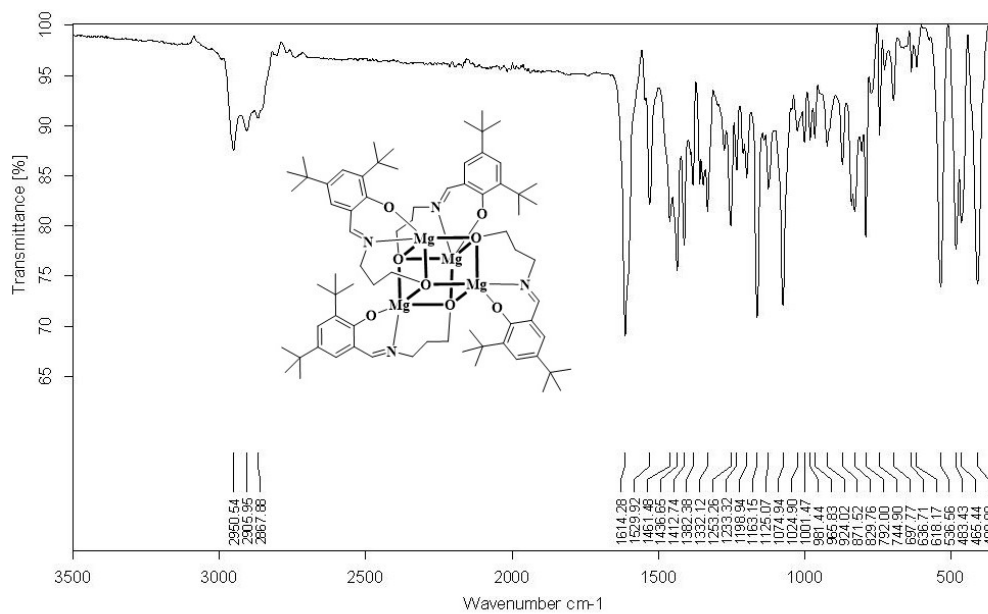
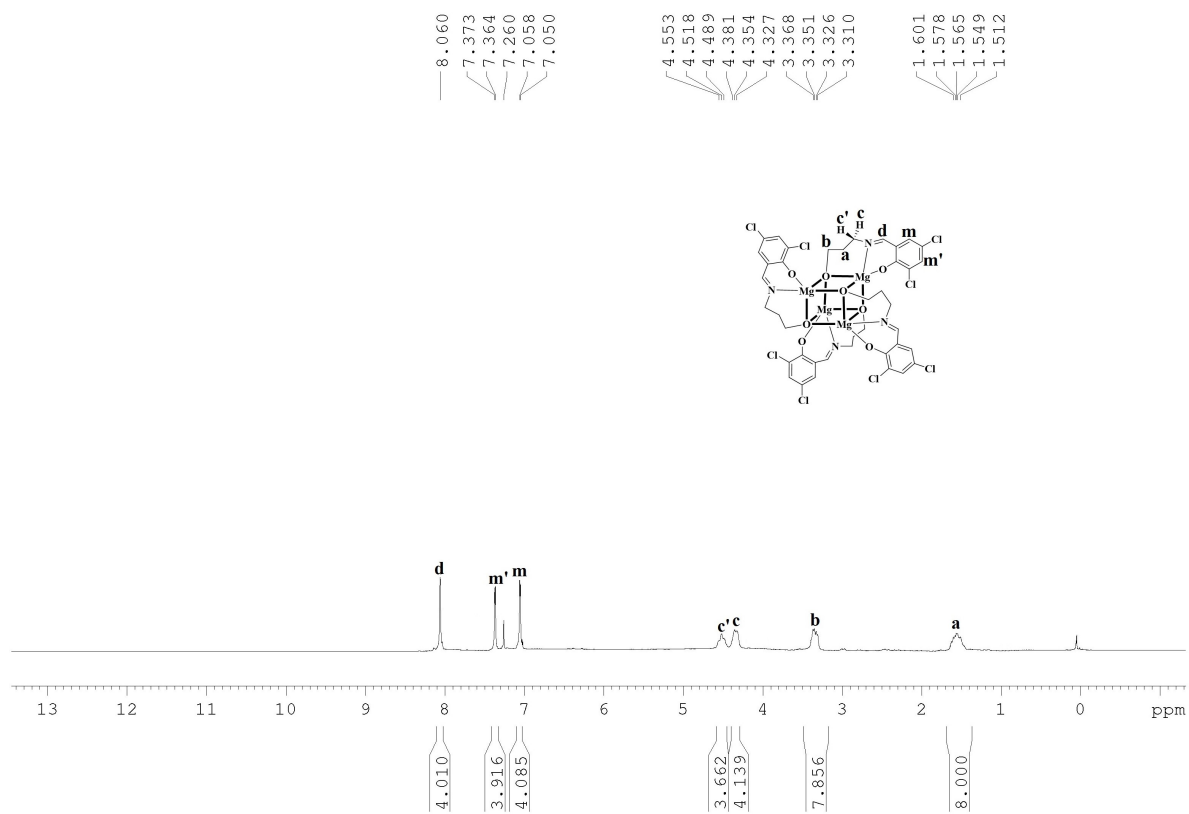
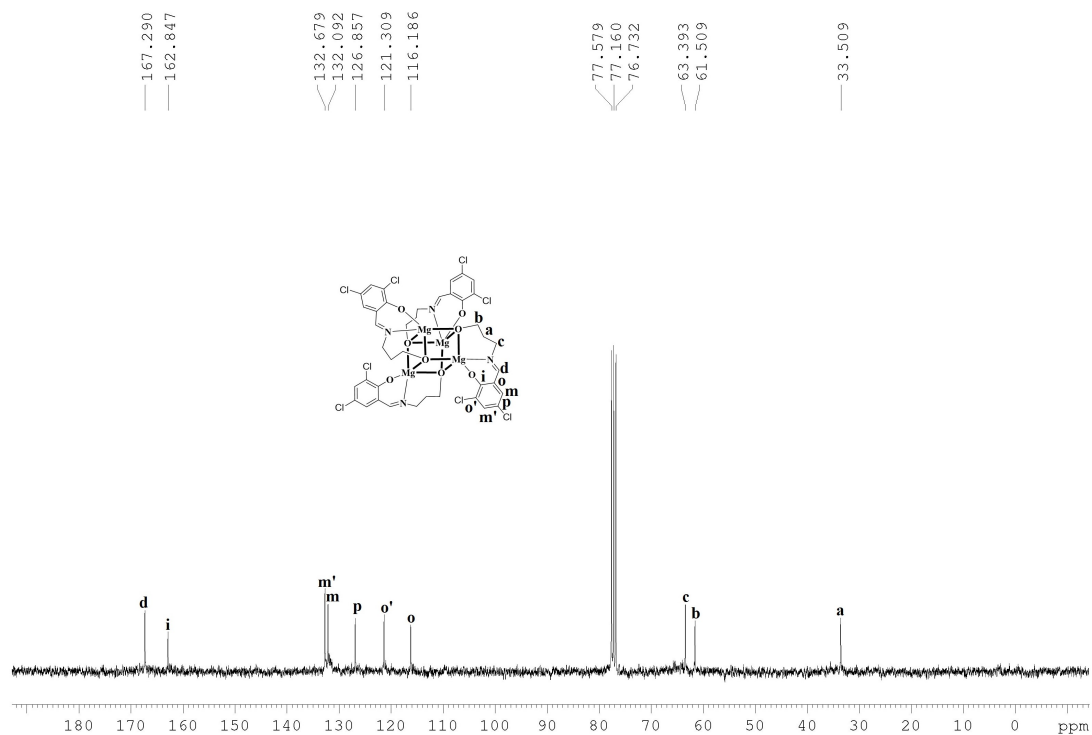


Figure S4. <sup>1</sup>H NMR (300 MHz, CDCl<sub>3</sub>, 25 °C) spectrum of 2.



**Figure S5.**  $^{13}\text{C}$  NMR (75 MHz,  $\text{CDCl}_3$  25  $^\circ\text{C}$ ) spectrum of **2**.



**Figure S6.** IR spectrum of **2**.

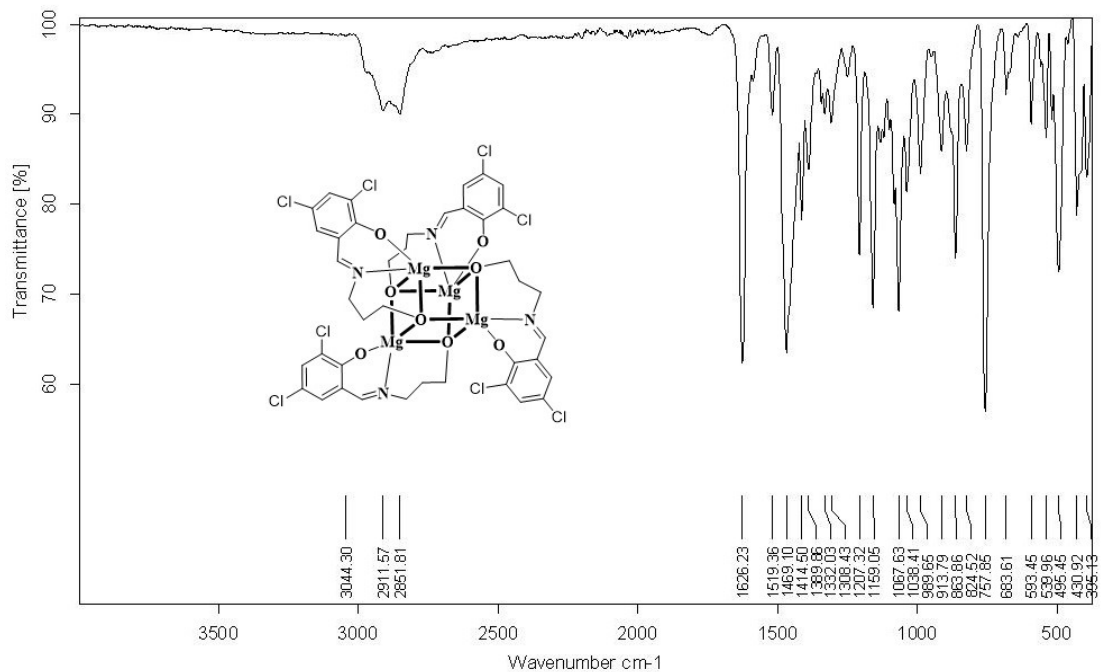


Figure S7.  $^1\text{H}$  NMR (300 MHz, Toluene- $d_8$ , 25  $^\circ\text{C}$ ) spectrum of **3**.

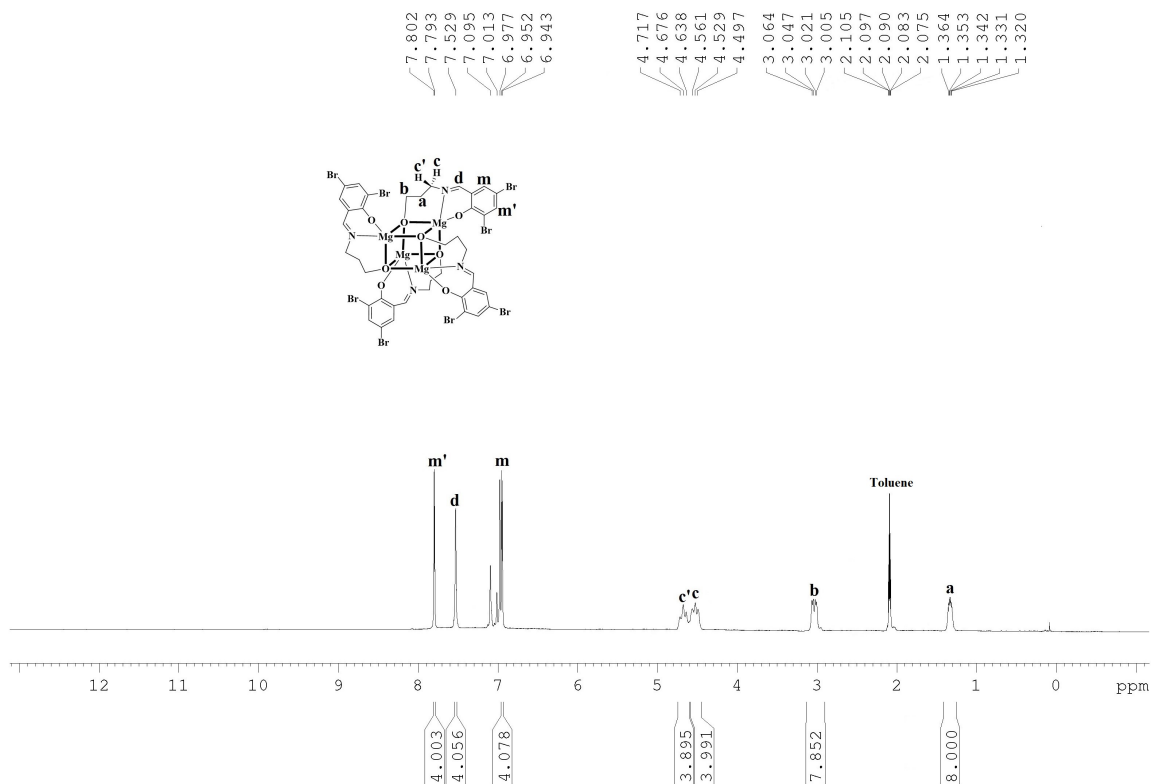


Figure S8.  $^{13}\text{C}$  NMR (75 MHz, Toluene- $d_8$ , 25  $^\circ\text{C}$ ) spectrum of **3**.

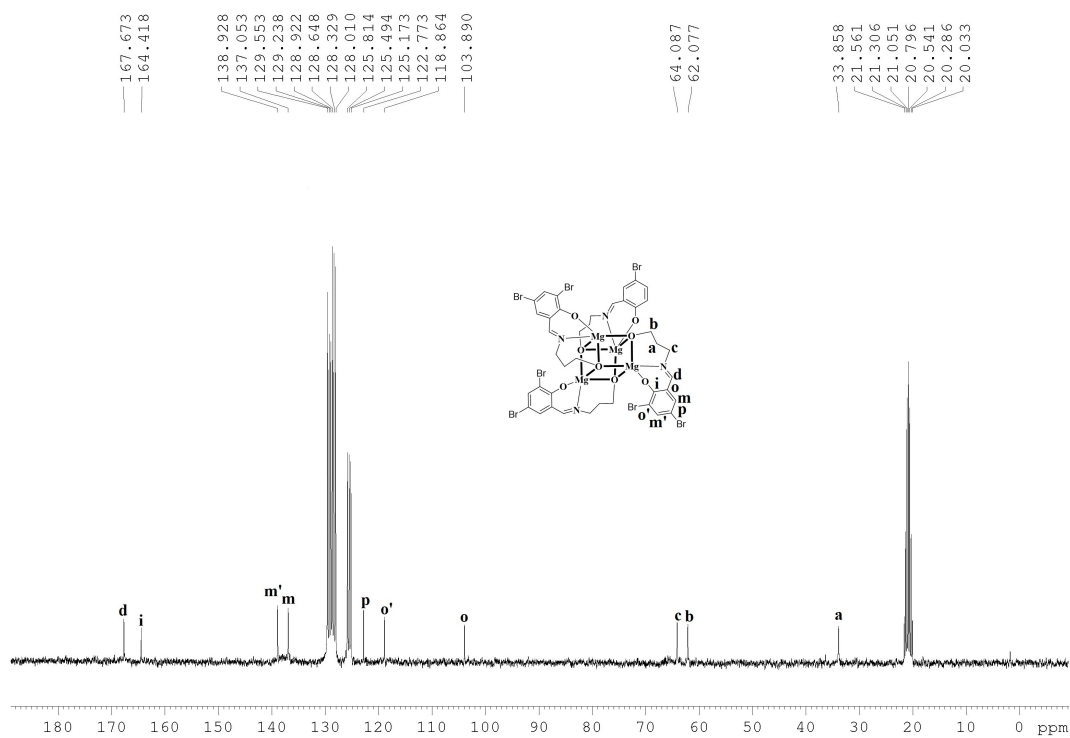


Figure S9. IR spectrum of 3.

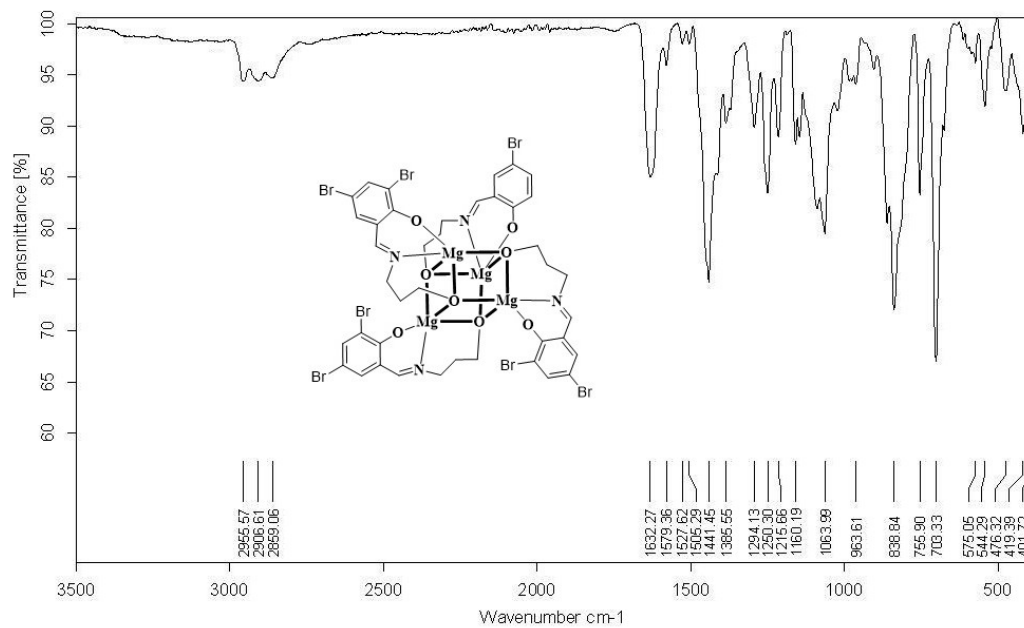
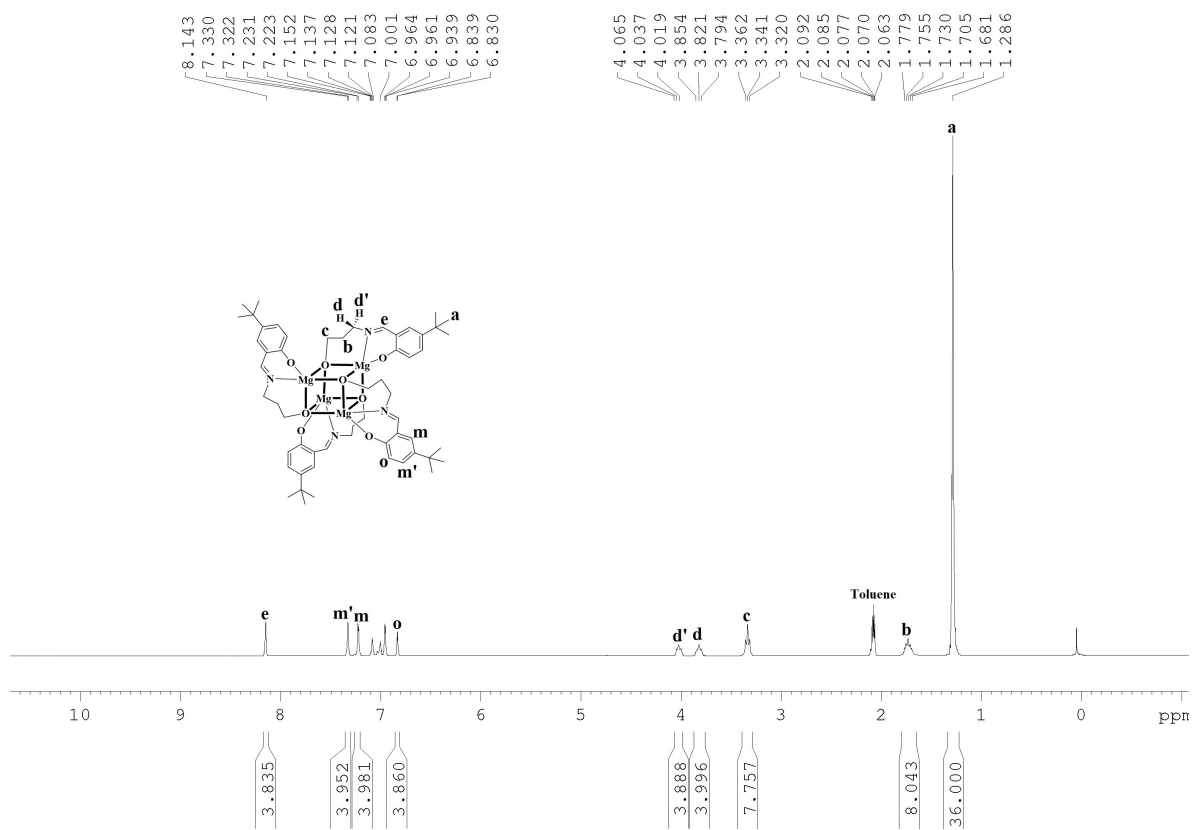
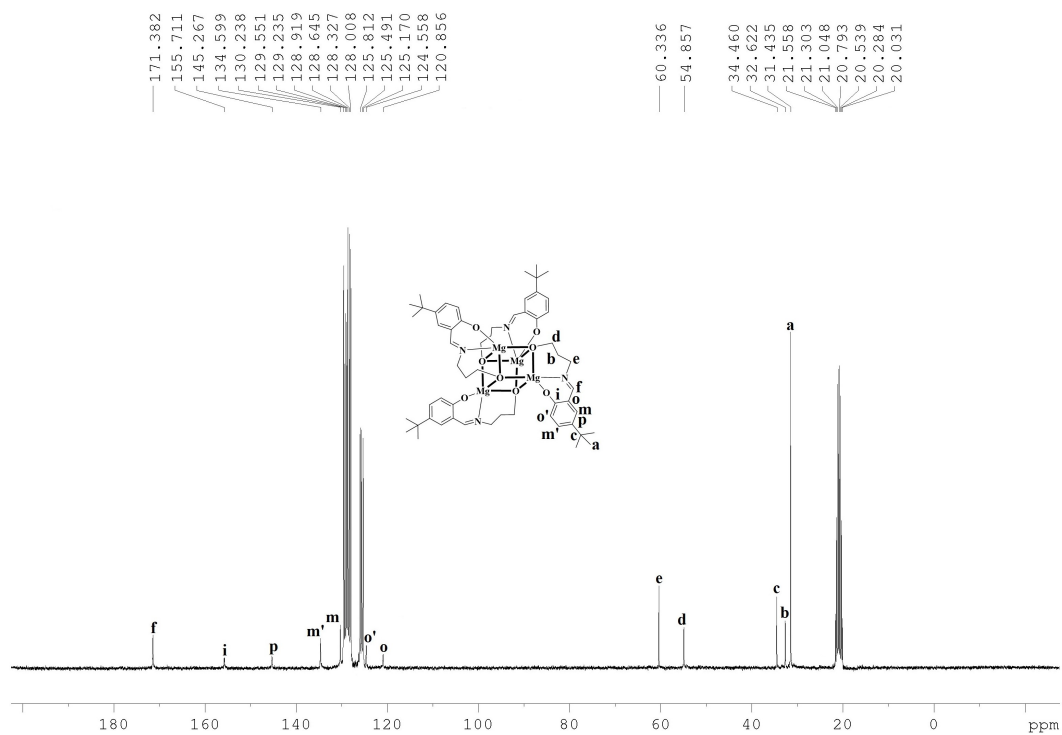


Figure S10. <sup>1</sup>H NMR (300 MHz, Toluene-d<sub>8</sub>, 25 °C) spectrum of 4.



**Figure S11.**  $^{13}\text{C}$  NMR (75 MHz, Toluene- $d_8$ , 25 °C) spectrum of **4**.



**Figure S12.** IR (300 MHz, Toluene- $d_8$ , 25 °C) spectrum of **4**.

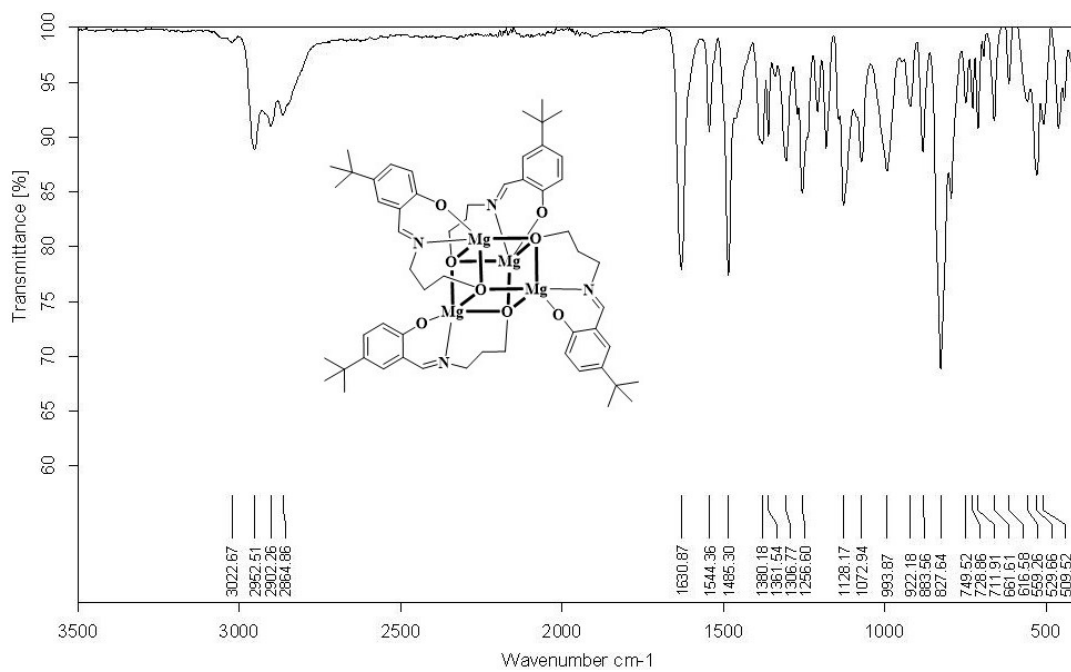


**Figure S13.** DOSY spectrum of (300 MHz, CDCl<sub>3</sub>, 25 °C) spectrum of **1**.

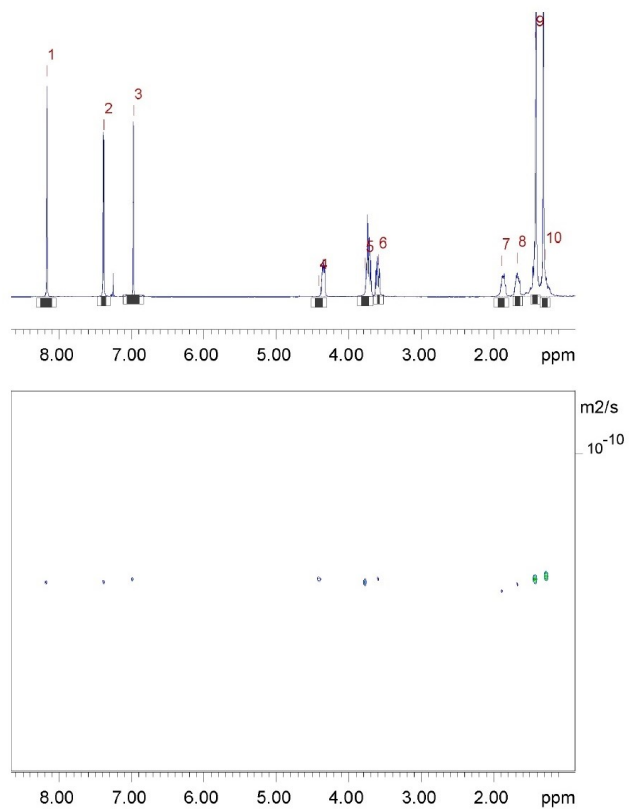


**Figure S14.** DOSY spectrum of (300 MHz, THF-d<sub>8</sub>, 25 °C) spectrum of **2**.

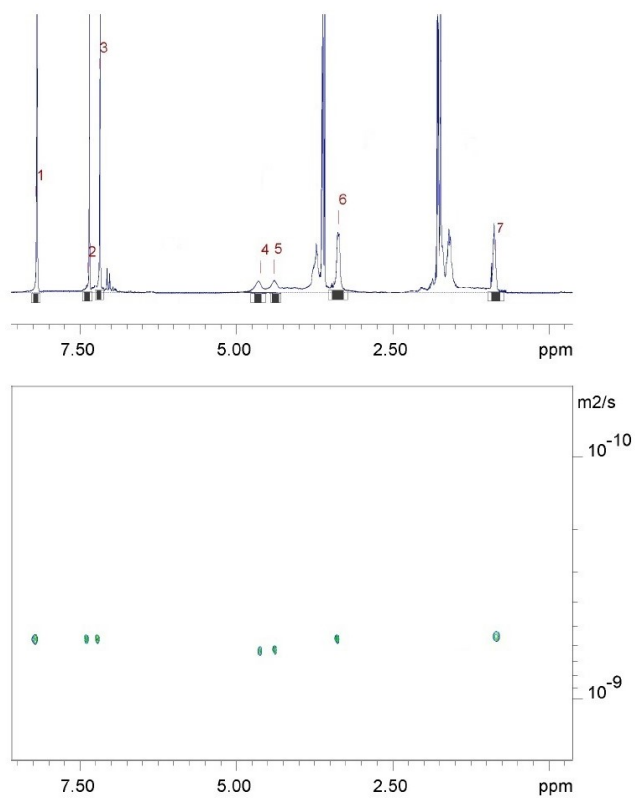


**Figure S15.** DOSY spectrum of (300 MHz, Toluene-d<sub>8</sub>, 25 °C) spectrum of **3**.

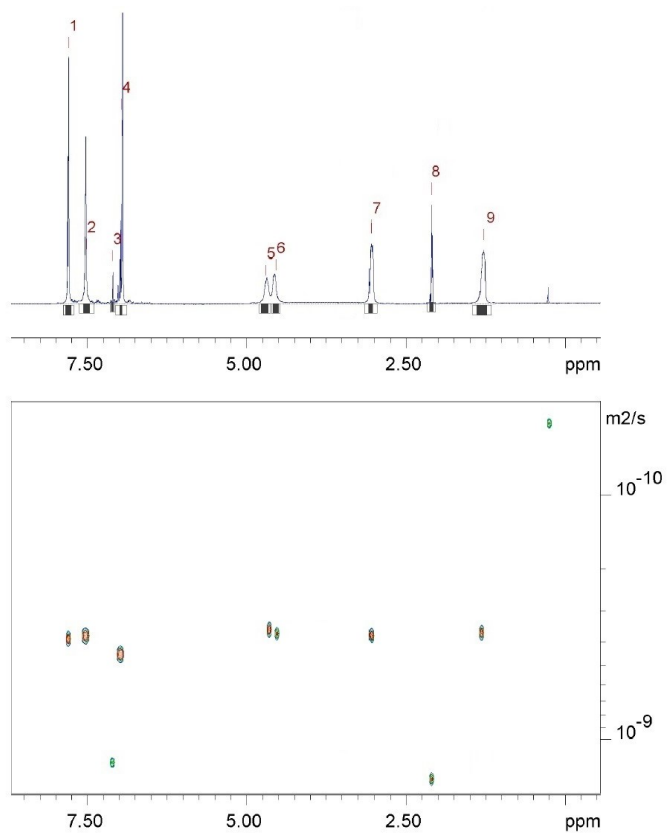
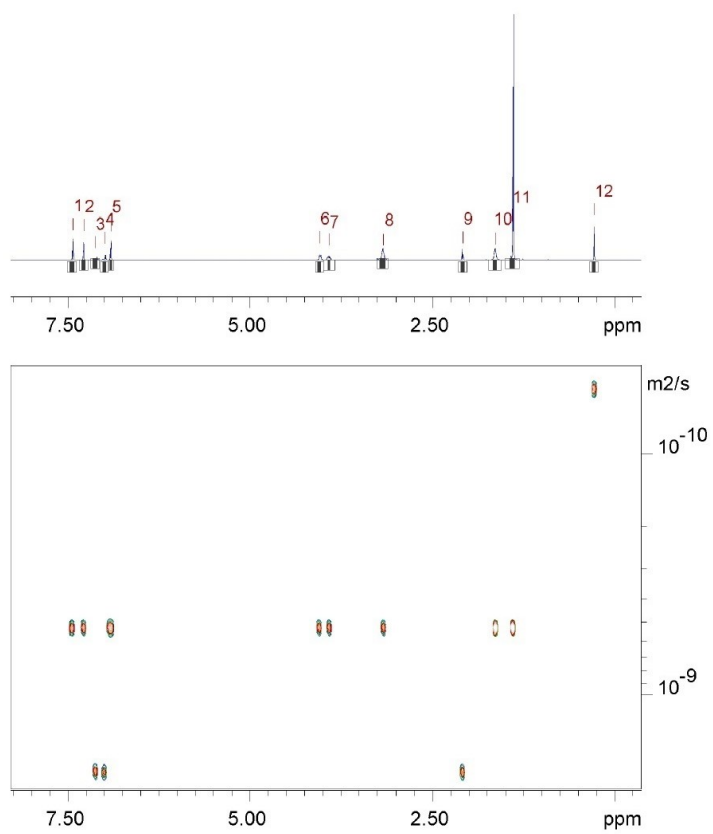


**Figure S16.** DOSY spectrum of (300 MHz, Toluene-d<sub>8</sub>, 25 °C) spectrum of **4**.



## II. Crystallographic Details

**Table S1.** Crystallographic data for compound **1**, **2**, **3** and **4**.

Compounds	<b>1</b>	<b>2·THF</b>	<b>3·THF</b>	<b>4·THF</b>
Empirical formula	C <sub>93</sub> H <sub>132</sub> Mg <sub>4</sub> N <sub>4</sub> O <sub>8</sub>	C <sub>64</sub> H <sub>84</sub> Cl <sub>8</sub> Mg <sub>4</sub> N <sub>4</sub> O <sub>14</sub>	C <sub>64</sub> H <sub>84</sub> Br <sub>8</sub> Mg <sub>4</sub> N <sub>4</sub> O <sub>14</sub>	C <sub>80</sub> H <sub>124</sub> Mg <sub>4</sub> N <sub>4</sub> O <sub>14</sub>
Formula weight (Da)	1531.26	1514.19	1869.87	1463.06
<i>T</i> /K	100(2)	100(2)	100(2)	100(2)
Wavelength (Å)	0.71073	0.71073	0.71073	0.71073
Crystal system,	monoclinic	tetragonal	orthorhombic	monoclinic
Space group	<i>Pc</i>	<i>P4</i> <sub>3</sub>	<i>Pna21</i>	<i>P2</i> <sub>1</sub> / <i>c</i>
<i>a</i> /Å	11.1710(13)	15.6933(9)	14.6910(13)	11.1387(7)
<i>b</i> /Å	15.5751(19)	15.6933(9)	21.9463(18)	20.3990(13)
<i>c</i> /Å	26.121(3)	28.4979(19)	22.8370(18)	17.5736(11)
<i>α</i> (°)	90	90	90	90
<i>β</i> (°)	102.316(7)	90	90	91.793(4)
<i>γ</i> (°)	90	90	90	90
<i>V</i> (Å <sup>3</sup> )	4440.2(9)	7018.5(9)	7362.9(11)	3991.1(4)
<i>Z</i> ,	2	4	4	2
Calc. density (g cm <sup>-3</sup> )	1.145	1.433	1.687	1.217
Abs. coef. (mm <sup>-1</sup> )	0.097	0.422	4.454	0.110
Crystal size (mm)	0.287 × 0.140 × 0.084	0.277 × 0.254 × 0.178	0.160 × 0.150 × 0.070	0.266 × 0.110 × 0.052
Θ range data collect. (°)	1.866- 33.219	1.429- 33.256	1.287°- 28.351°	1.530- 28.282
Refl. collected	105877	197302	153221	71773
Ind. refl.	30207	26563	18268	9730
Data/restraints/parameters	18046/1103/1010	21850/1285/979	12006/1495/1051	6143/285/530
Flack-Parameter <i>x</i>	-0.11(11)	see comment	0.056(3)	–
Goodness-of-fit on <i>F</i> <sup>2</sup>	1.027	1.027	1.055	1.037
Final <i>R</i> indices [ <i>I</i> > 2σ( <i>I</i> )]	<i>R</i> 1 = 0.0817	<i>R</i> 1 = 0.0488	<i>R</i> 1 = 0.0455	<i>R</i> 1 = 0.0578
	<i>wR</i> 2 = 0.1634	<i>wR</i> 2 = 0.1132	<i>wR</i> 2 = 0.0922	<i>wR</i> 2 = 0.1314
<i>R</i> indices (all data)	<i>R</i> 1 = 0.1564	<i>R</i> 1 = 0.0709	<i>R</i> 1 = 0.0927	<i>R</i> 1 = 0.1107
	<i>wR</i> 2 = 0.1992	<i>wR</i> 2 = 0.1262	<i>wR</i> 2 = 0.1033	<i>wR</i> 2 = 0.1600

**Table S2.** Mg-O and Mg-N bond lengths as well as O-Mg-O and Mg-O-Mg bond angles of compound **1**, **2**[thf]<sub>2</sub>, **3**[thf]<sub>2</sub> and **4**[thf]<sub>2</sub>.

	<b>1</b>	<b>2</b> [thf] <sub>2</sub>	<b>3</b> [thf] <sub>2</sub>	<b>4</b> [thf] <sub>2</sub>
<b>Mg-O<sub>endo</sub></b>	2.042(5)	2.015(3)	2.056(5)	1.9808(17)
	2.073(5)	2.033(3)	2.063(5)	1.9937(16)
	2.073(5)	2.077(3)	2.192(5)	2.0698(15)
	2.046(5)	1.958(3)	2.051(6)	2.0069(16)
	2.053(5)	2.065(3)	2.073(5)	2.0654(16)
	2.060(5)	2.167(3)	2.020(5)	2.1010(16)
	2.042(5)	2.039(3)	2.035(5)	2.1096(16)
	2.044(5)	2.048(3)	2.165(5)	
	2.076(5)	2.053(3)	2.043(5)	
	2.046(5)	2.046(3)	2.071(5)	
	2.060(5)	2.081(3)	2.055(5)	
	2.063(5)	2.166(3)	2.039(5)	
<b>Mg-O<sub>exo</sub></b>	1.928(5)	1.938(3)	1.946(5)	1.9373(16)
	1.915(5)	1.958(3)	1.927(5)	
	1.936(5)	1.932(3)	1.952(5)	
	1.922(5)	1.953(3)	1.943(5)	
<b>Mg-N</b>	2.120(7)	2.142(3)	2.157(6)	2.1725(19)
	2.120(6)	2.161(4)	2.147(7)	2.166(2)
	2.114(6)	2.152(4)	2.147(6)	
	2.119(6)	2.154(3)	2.171(6)	
<b>O-Mg-O<sub>endo</sub></b>	84.9(2)	86.41(11)	84.18(18)	106.95(7)
	84.5(2)	84.98(11)	81.73(19)	81.75(6)
	84.2(2)	85.21(12)	81.6(2)	83.30(6)
	85.4(2)	84.16(11)	86.1(2)	99.53(7)
	83.0(2)	81.42(11)	85.4(2)	176.00(7)
	84.2(2)	81.73(11)	84.46(19)	80.83(6)
	85.7(2)	85.82(11)	84.23(19)	80.16(6)
	84.8(2)	85.22(11)	82.7(2)	84.77(6)
	82.7(2)	85.27(11)	81.61(19)	103.83(6)
	84.7(2)	84.59(11)	85.5(2)	
	84.3(2)	81.75(11)	84.74(19)	
	84.8(2)	81.43(11)	85.3(2)	

<b>O–Mg–O<sub>exo</sub></b>	107.4(2)	162.81(14)	98.1(2)	141.91(8)
	94.8(2)	110.34(13)	177.6(2)	110.60(7)
	168.0(2)	92.36(12)	99.4(2)	96.31(6)
	102.0(2)	98.27(12)	108.4(2)	
	93.8(2)	177.38(13)	164.8(3)	
	174.4(2)	99.54(12)	92.4(2)	
	93.3(2)	113.07(13)	179.9(3)	
	100.1(2)	161.07(14)	95.7(2)	
	176.5(2)	94.76(12)	97.4(2)	
	105.9(2)	178.71(14)	163.3(3)	
	169.2(2)	96.28(12)	111.2(2)	
	94.5(2)	97.43(12)	96.7(2)	
<b>Mg–O–Mg</b>	95.9(2)	95.92(12)	98.4(2)	102.08(7)
	94.9(2)	94.78(12)	93.3(2)	97.90(7)
	94.7(2)	97.94(12)	94.6(2)	96.65(6)
	97.3(2)	98.14(12)	95.9(2)	95.23(6)
	94.3(2)	93.83(12)	94.2(2)	95.79(6)
	95.1(2)	93.91(11)	97.7(2)	
	95.0(2)	94.87(12)	95.3(2)	
	96.7(2)	96.89(12)	97.3(2)	
	93.8(2)	94.09(12)	94.3(2)	
	95.8(2)	94.99(12)	95.3(2)	
	95.5(2)	98.35(12)	97.6(2)	
	94.4(2)	94.51(11)	94.9(2)	

### III. Polymerization Studies

**Figure S17.** Homonuclear decoupled  $^1\text{H}$ -NMR spectrum of *rac*-PLA in  $\text{CDCl}_3$  (methine H-atom region) obtained by reaction of *rac*-LA and **1** in 200:1 molar ratio at 140 °C.

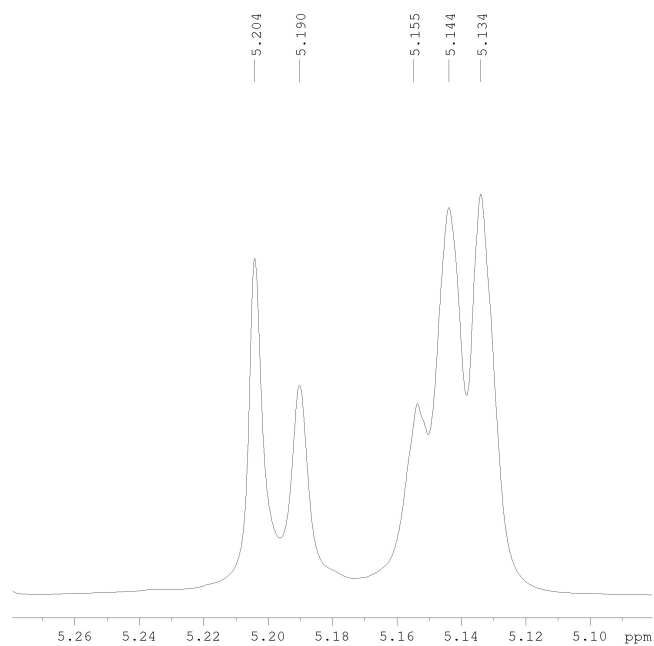


**Figure S18.** Homonuclear decoupled  $^1\text{H}$ -NMR spectrum of *rac*-PLA in  $\text{CDCl}_3$  (methine H-atom region) obtained by reaction of *rac*-LA and **2** in 200:1 molar ratio at 140 °C.

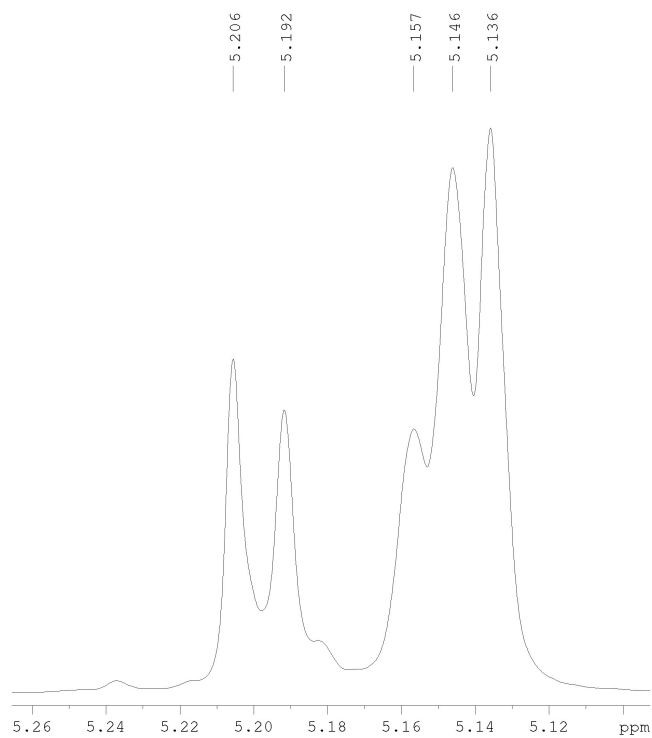


**Figure S19.** Homonuclear decoupled  $^1\text{H-NMR}$  spectrum of *L*-PLA in  $\text{CDCl}_3$  (methine H-atom region) obtained by reaction of *L*-LA and **1** in 200:1 molar ratio at 140 °C.

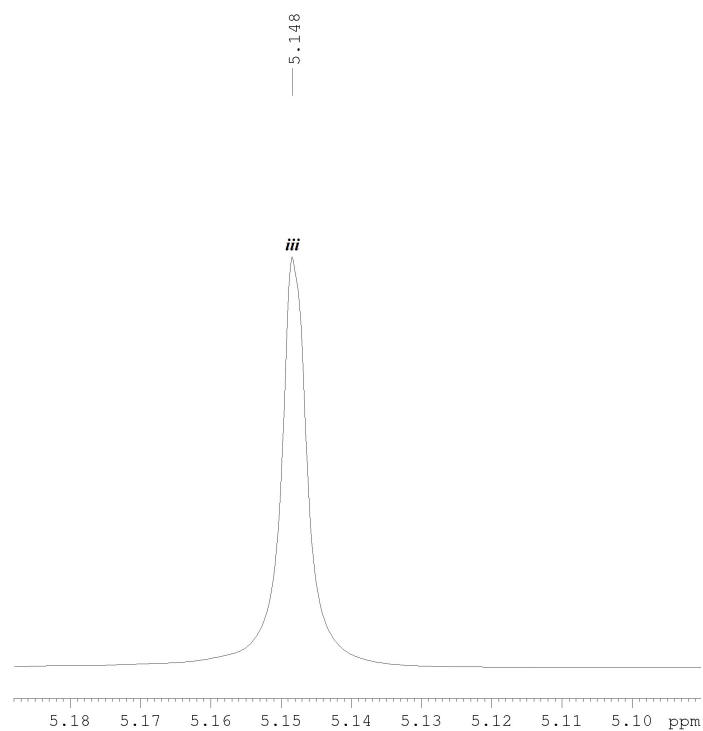


**Figure S20.**  $^1\text{H-NMR}$  spectrum of *rac*-PLA in  $\text{CDCl}_3$  obtained by reaction of *rac*-LA and **1** in 50:1 molar ratio at 140 °C.

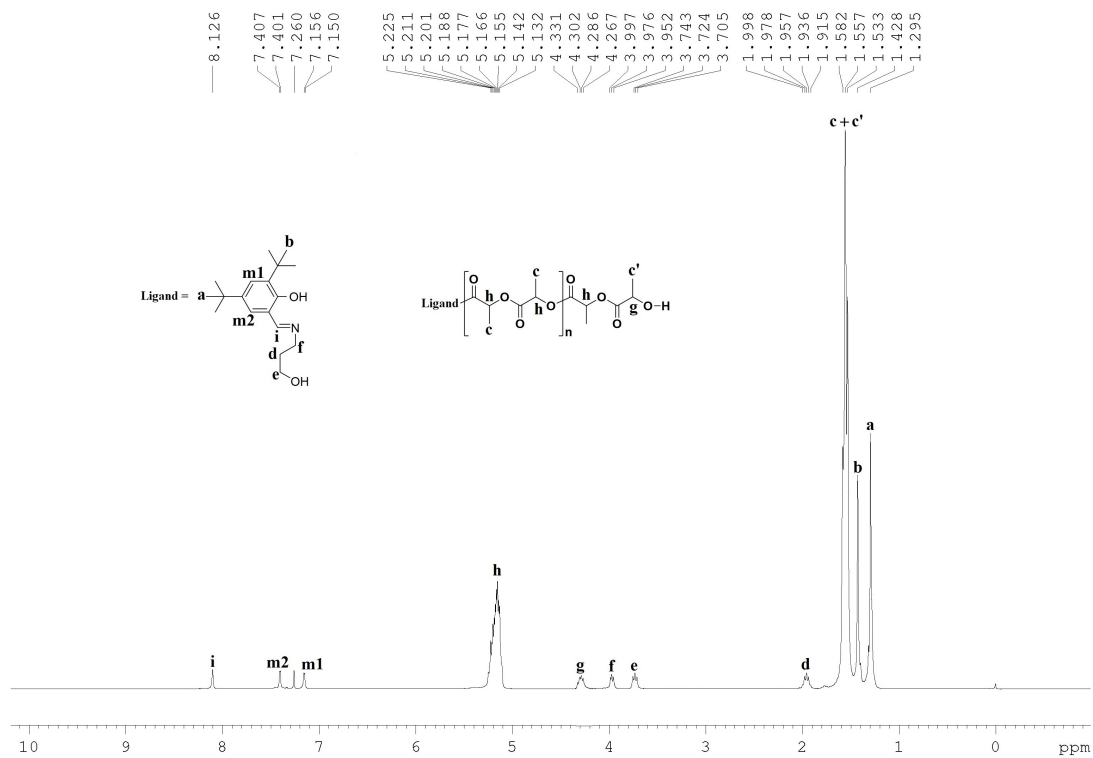


**Figure S21.** MALDI-TOF spectrum of *rac*-PLA obtained by reaction of *rac*-LA and **1** in 50:1 molar ratio at 140 °C.

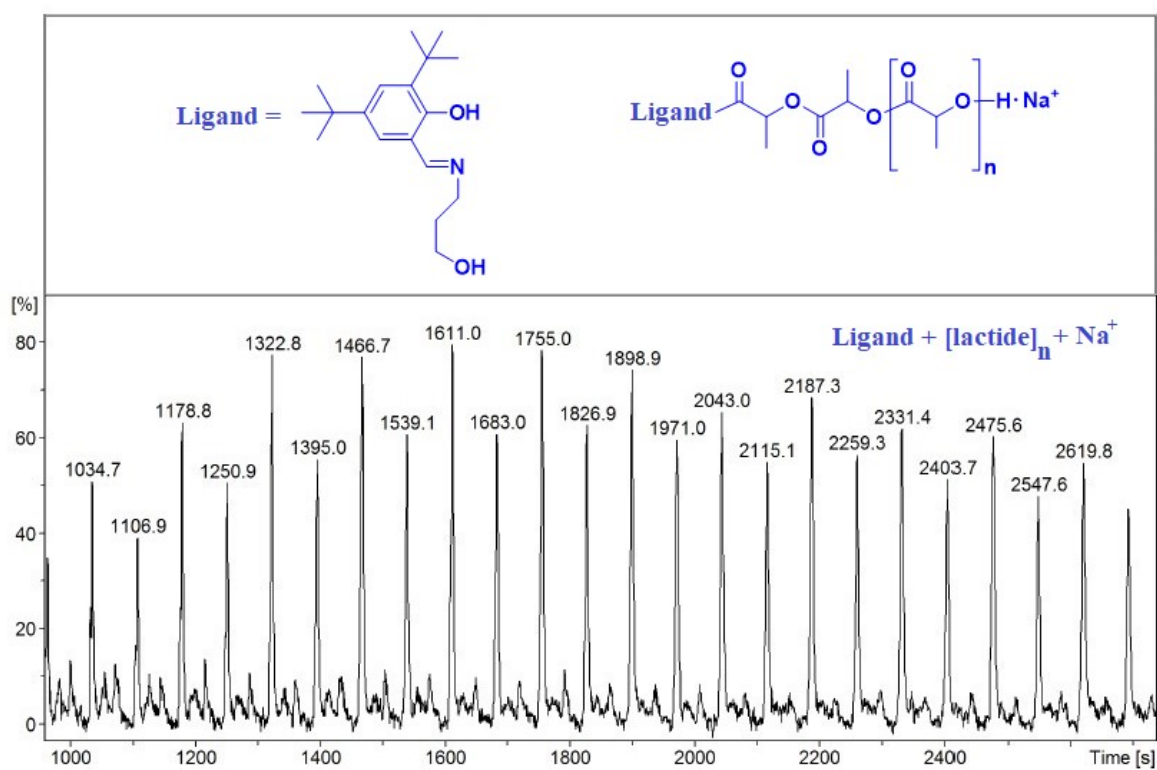


**Figure S22.** <sup>1</sup>H-NMR spectrum of  $\epsilon$ -PCL in CDCl<sub>3</sub> obtained by reaction of  $\epsilon$ -CL and **1** in 50:1 molar ratio at 80 °C.

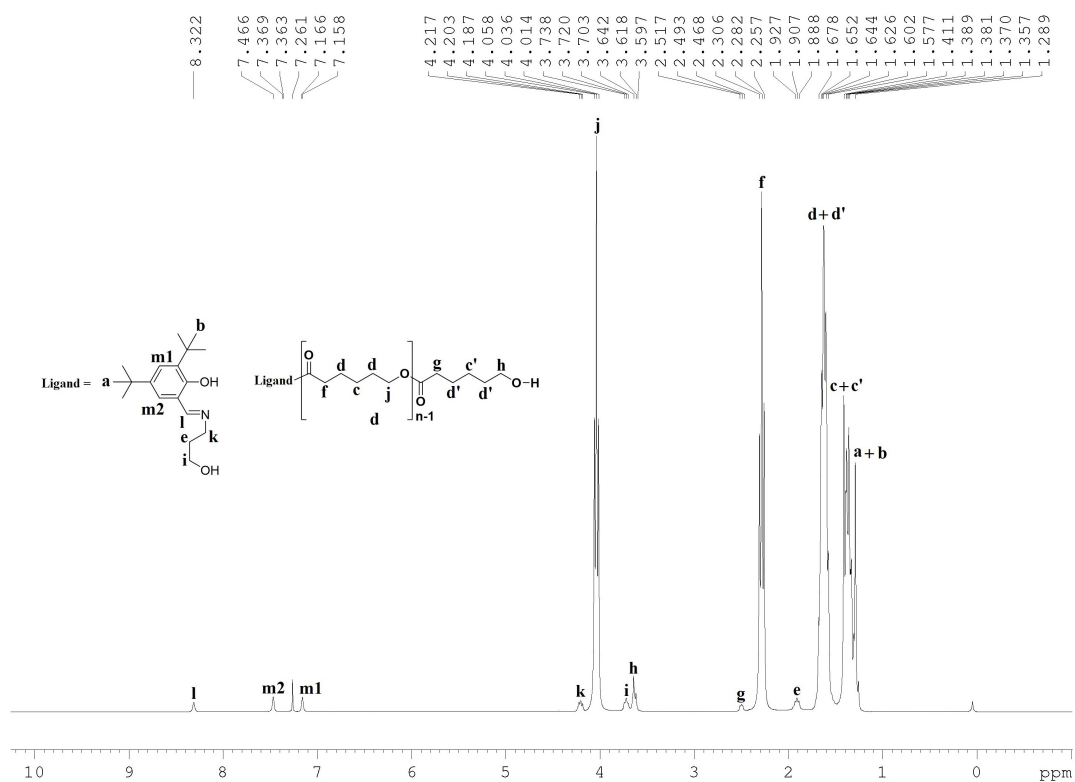


**Figure S23.** MALDI-TOF spectrum of  $\epsilon$ -PCL in  $\text{CDCl}_3$  obtained by reaction of  $\epsilon$ -CL and **1** in 50:1 molar ratio at 80 °C.

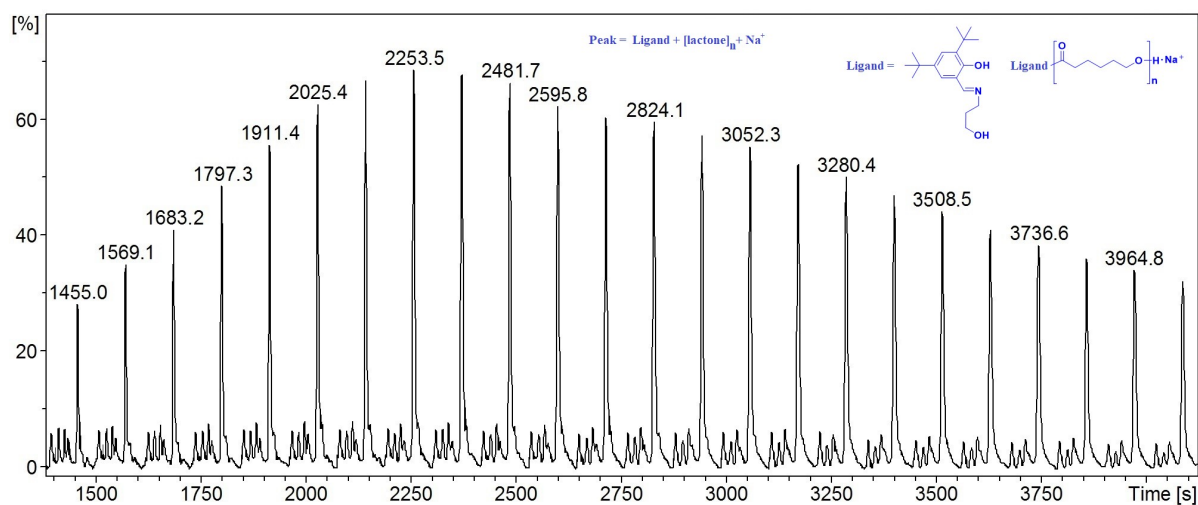


**Figure S24.** <sup>1</sup>H-NMR spectrum of *rac*-PLA in  $\text{CDCl}_3$  obtained by reaction of *rac*-LA and **1** in the presence of benzyl alcohol as a co-initiator in 50:1:2 molar ratio at 140 °C.

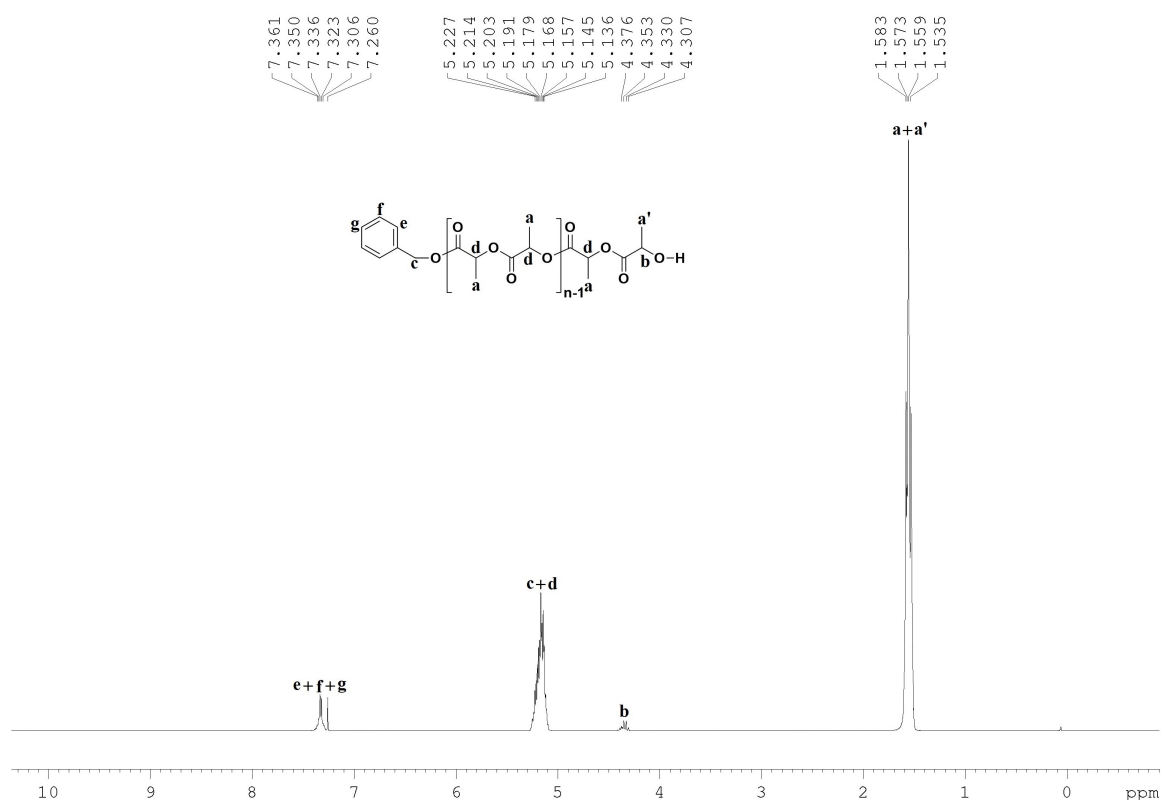




**Figure S27.** MALDI-TOF spectrum of  $\epsilon$ -PCL in  $\text{CDCl}_3$  obtained by reaction of  $\epsilon$ -CL and **1** in the presence of benzyl alcohol as a co-initiator in 50:1:2 molar ratio at 80 °C.

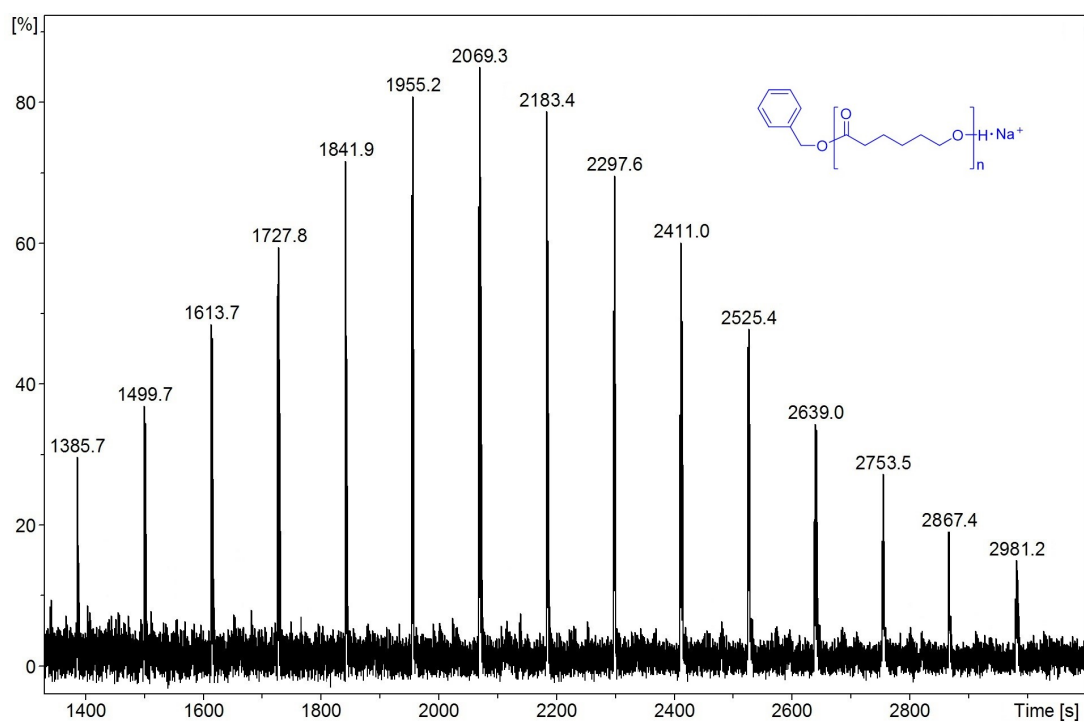


**Figure 28.** IR spectrum of *rac*-PLA obtained by reaction of *rac*-LA and **1** in 50:1 molar ratio at 140 °C.

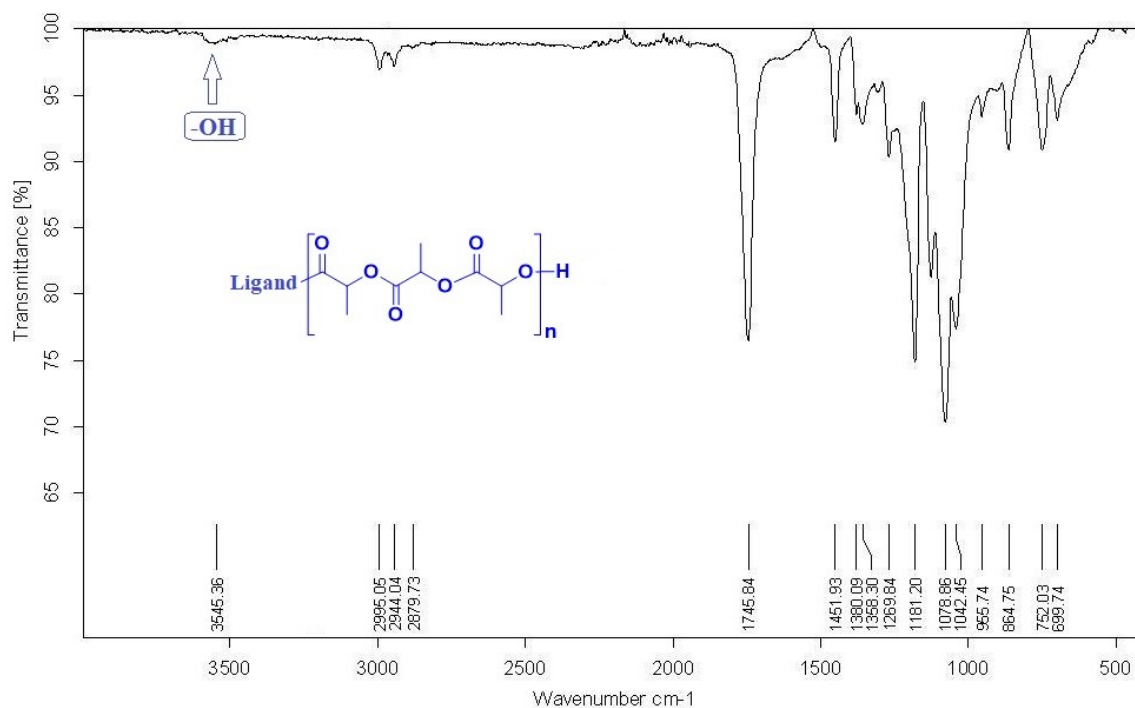


**Figure 29.** IR spectrum of  $\epsilon$ -PCL obtained by reaction of  $\epsilon$ -CL and **1** in 50:1 molar ratio at 80 °C.

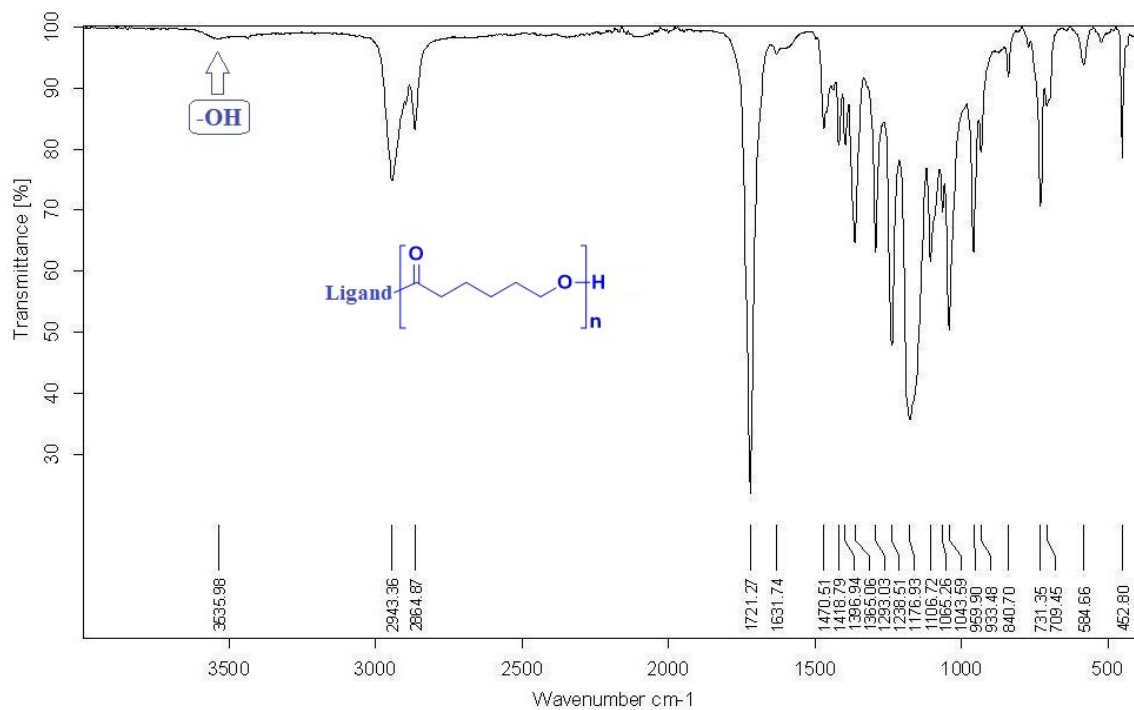


**Figure 30.** GPC diagram of *rac*-PLA obtained by reaction of *rac*-LA and **1** in 2000:1 molar ratio at 140 °C.

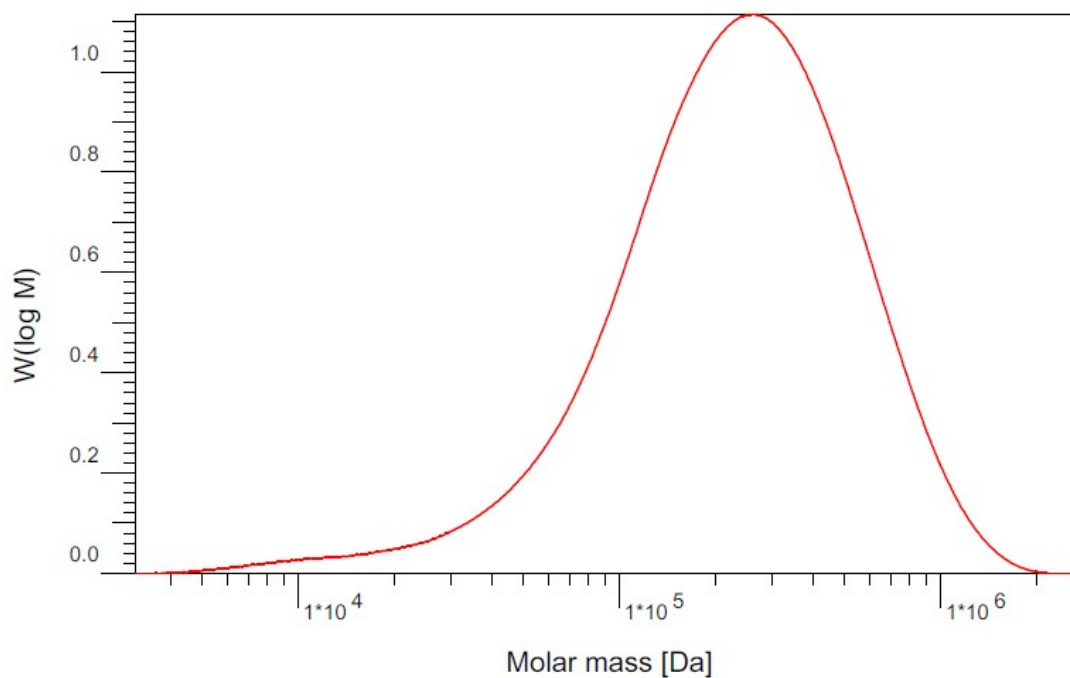


**Figure 31.** GPC diagram of *rac*-PLA obtained by reaction of *rac*-LA and **1** in 10000:1 molar ratio at 140 °C.

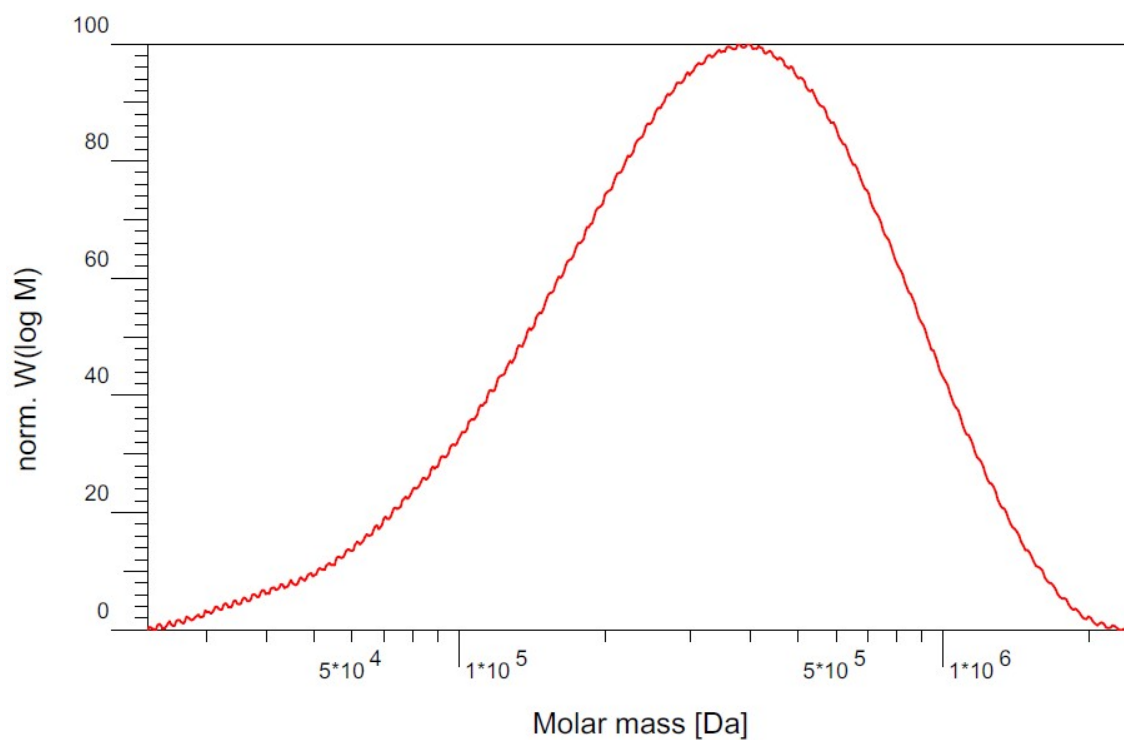


**Figure 32.** GPC diagram of  $\epsilon$ -PCL obtained by reaction of  $\epsilon$ -CL and **1** in 5000:1 molar ratio at 80 °C.

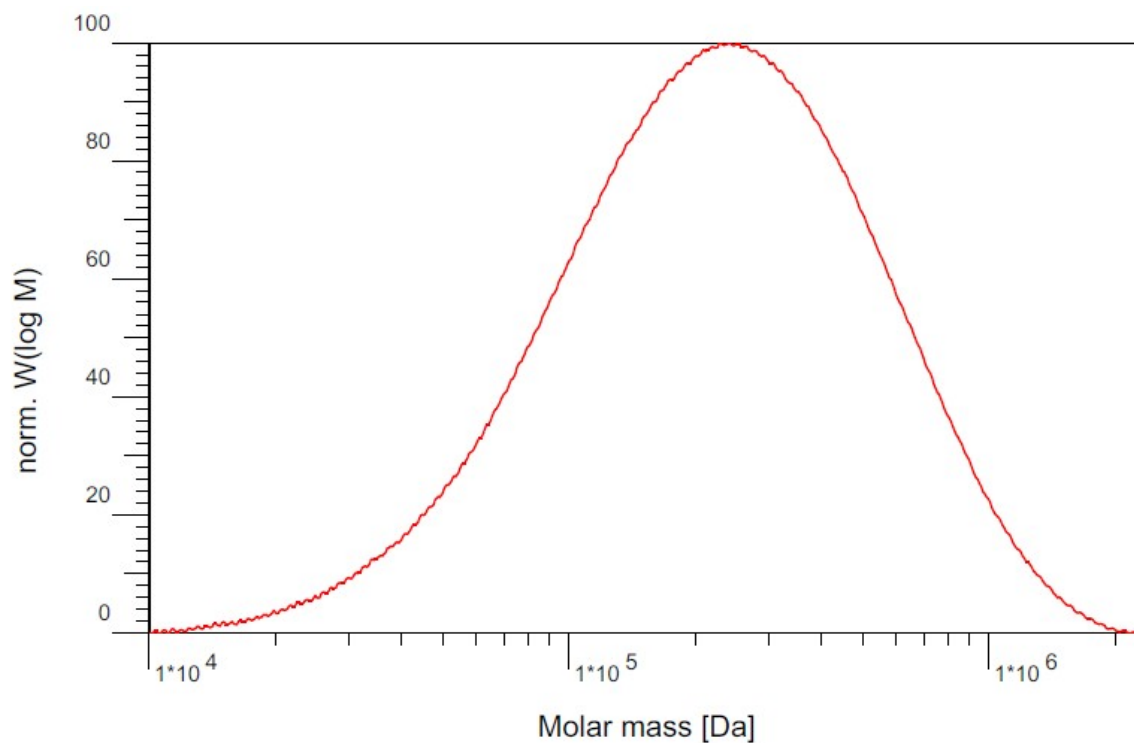


**Figure 33.** GPC diagram of  $\epsilon$ -PCL obtained by reaction of  $\epsilon$ -CL and **1** in 10000:1 molar ratio at 80 °C.

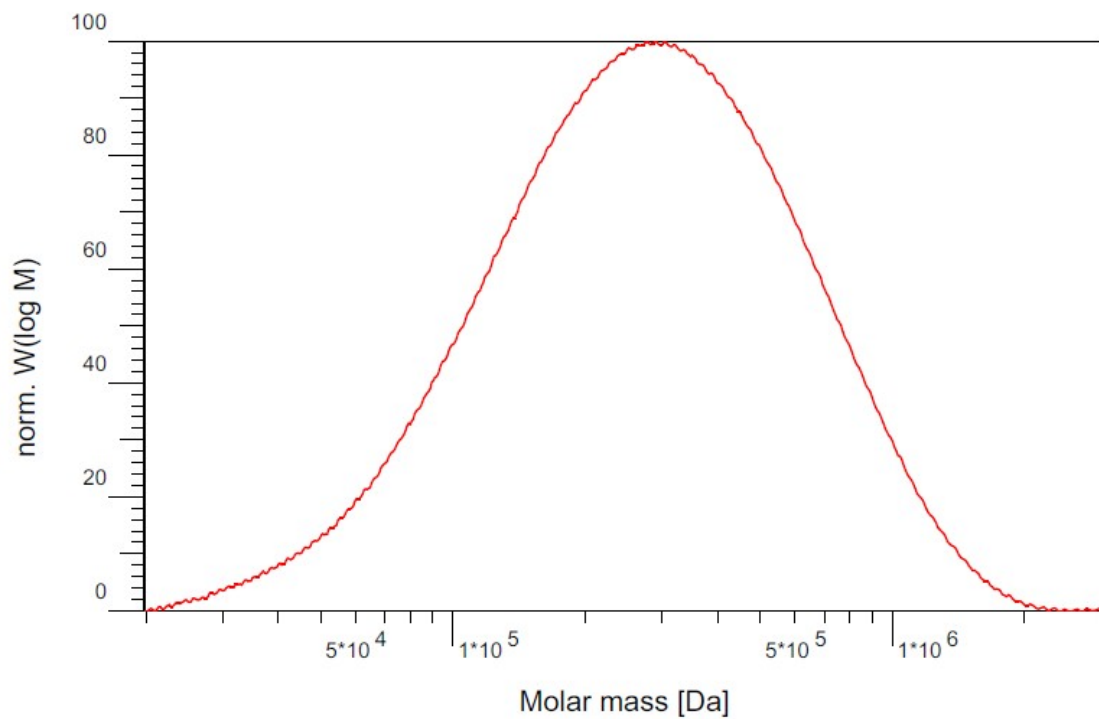


**Table S3.** Polymerization data for *rac*-LA and  $\epsilon$ -CL with **1-4** with BnOH as an initiator in 200:1:4 ratios at the solvent free condition.

Entry	Catalyst	Monomer	Temp ° C	Time <sup>a</sup> (s)	Conv <sup>b</sup> %	$M_n^{(Obs)c}$ (kg/mol)	$M_n^{(Theo)d}$ (kg/mol)	$M_n^{(NMR)e}$ (kg/mol)	$M_w/M_n$
1	<b>1</b>	<i>rac</i> -LA	140	150	97	6.33	7.10	6.50	1.1
2	<b>2</b>	<i>rac</i> -LA	140	200	95	5.81	6.85	6.30	1.1
3	<b>3</b>	<i>rac</i> -LA	140	400	92	9.56	6.63	8.25	1.2
4	<b>4</b>	<i>rac</i> -LA	140	180	97	5.98	7.10	6.30	1.2
5	<b>1</b>	$\epsilon$ -CL	80	60	98	5.54	5.59	5.85	1.2
6	<b>2</b>	$\epsilon$ -CL	80	90	97	5.33	5.64	5.16	1.3
7	<b>3</b>	$\epsilon$ -CL	80	300	95	9.16	5.53	8.75	1.4
8	<b>4</b>	$\epsilon$ -CL	80	80	95	5.48	5.53	5.10	1.3

<sup>a</sup>Time of polymerization measured when quenching the polymerization reaction at complete conversion.

<sup>b</sup>Determined by <sup>1</sup>H NMR in CDCl<sub>3</sub>. <sup>c</sup>Measured by gel permeation chromatography at 40 °C in THF relative to polystyrene standards. <sup>d</sup>Theoretical mol. Wt. =  $[M]_0/[C]_0[BnOH]_0 \times \text{mol. Wt. (monomer)} \times \% \text{ conversion} + M_n^{\text{end groups}}$ . <sup>e</sup>Determined by <sup>1</sup>H NMR in CDCl<sub>3</sub>.

**Table S4.** Polymerization data of *rac*-LA and  $\epsilon$ -CL using catalyst **1** with varying  $[M]_0/[C]_0$

Entry	Monomer	$[M]_0/[C]_0$	Temp (° C)	Time <sup>a</sup> (s)	Yield <sup>b</sup> (%)	$M_n^{(obs)c}$ (kg/mol)	$M_n^{(Theo)d}$ (kg/mol)	$M_w/M_n$
1	<i>rac</i> -LA	200:1	140	175	96	13.8	28.8	1.4
2	<i>rac</i> -LA	400:1	140	290	95	26.1	57.5	1.5
3	<i>rac</i> -LA	600:1	140	400	95	40.9	86.4	1.6
4	<i>rac</i> -LA	800:1	140	610	92	54.2	115.3	1.8
5	<i>rac</i> -LA	1000:1	140	730	90	66.4	144.1	1.8
6	<i>rac</i> -LA	400 (400):1	140	320 (320)	90	51.1	115.3	1.8
7	$\epsilon$ -CL	200:1	80	70	98	14.1	22.8	1.3
8	$\epsilon$ -CL	400:1	80	155	98	26.8	45.6	1.4
9	$\epsilon$ -CL	600:1	80	190	96	38.2	68.4	1.3
10	$\epsilon$ -CL	800:1	80	240	95	51.1	91.2	1.4
11	$\epsilon$ -CL	1000:1	80	290	95	62.3	114.0	1.5
12	$\epsilon$ -CL	2000:1	80	380	92	125.5	228.0	1.8
13	$\epsilon$ -CL	400 (400):1	80	120 (120)	94	53.4	91.2	1.6

<sup>a</sup>Time required for complete conversion. <sup>b</sup>Isolated yield of the polymer after quenching. <sup>c</sup>Measured by GPC at 40 °C in THF, relative to polystyrene standards. <sup>d</sup> $M_n^{(Theo)}$  at 100% conversion =  $[M]_0/[C]_0 \times \text{mol. Wt. of monomer}$ .